

# Simulation and Energy Optimization of Ammonia Synthesis Loop

Ashutosh Desai<sup>#1</sup>, Shreyans Shah<sup>#2</sup>, Sanchit Goyal<sup>#3</sup>

Under the guidance of,  
Prof. Arvind Prasad

Department of chemical engineering, Dwarkadas.J.Sanghavi college of Engineering,  
Plot U-15, Bhaktivedanta swami marg, Ville parle (W), Mumbai-56, India.

## Abstract

In this study, a flow sheet representing Ammonia Synthesis Loop for industrial production of Ammonia referred from the literature has been optimized by proposing a rigorous kinetic model for a plug flow reactor. The kinetic model proposed is developed on Scilab and the flow sheet is simulated using Cape-Open to Cape-Open Simulator. Various output parameters and corresponding operational profits have been analysed for different input feed flow rates.

**Keywords:** ammonia, optimization, SciLab, reactor, modelling, simulation.

## I. INTRODUCTION

Industrial ammonia is sold either as ammonia liquor (usually 28% ammonia in water) or as pressurized or refrigerated anhydrous liquid ammonia transported in tank cars or cylinders. (Bland, 2015)

In most commercial plants, either steam reforming of methane or gasification of coal is used as the source of nitrogen and hydrogen gas for the Haber-Bosch synthesis loop. The nitrogen and hydrogen gas mixture, which is called synthetic gas, is first compressed to 120-220 bars, depending on the particular plant, before it enters the ammonia synthesis loop. Only a fraction of the synthetic gas is converted to ammonia in a single pass through the converter due to thermodynamic equilibrium of the ammonia synthesis reaction as shown



The converter typically contains a catalyst of iron promoted with K<sub>2</sub>O and Al<sub>2</sub>O<sub>3</sub> to speed the reaction and to increase the amount of ammonia produced during each pass. The gaseous ammonia and unconverted gas then enters the ammonia recovery portion of the synthesis loop. The Haber-Bosch process continues to be improved, mostly through changes in the catalyst and heat recovery. One catalytic improvement that is starting to be used commercially is a ruthenium-based catalyst instead of an iron-based catalyst. An improved catalyst allows more ammonia to be produced per pass through the converter at lower temperatures and pressures. As a

result, less energy is consumed in the production of ammonia.

## A. Kinetic Model

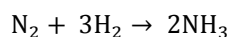
The rate expression of Temkin-Phyzhez has been widely accepted to represent the synthesis of ammonia over wide ranging conditions, a modified form of the Temkin-Phyzhez equation expressed in terms of activities as developed by (Dyson & Simon, 1968) was used in this work.

The rate expression is given by:

$$R_{\text{NH}_3} = 2k \left( K_a^2 a_{\text{N}_2} \left[ \frac{a_{\text{H}_2}^3}{a_{\text{NH}_3}^2} \right]^\alpha - \left[ \frac{a_{\text{NH}_3}^2}{a_{\text{H}_2}^3} \right]^{1-\alpha} \right) \quad (1)$$

Where k is the rate constant for the reverse reaction, K<sub>a</sub> is the equilibrium constant, a<sub>i</sub> is the activity of component i and α is a constant which takes a value from 0.5 to 0.75.

The rate equation for the reactants was determined using the stoichiometry of the reaction



And used to relate the individual rates of reaction as follows

$$\frac{R_{\text{N}_2}}{-1} = \frac{R_{\text{H}_2}}{-3} = \frac{R_{\text{NH}_3}}{2} \quad (2)$$

## B. Mass Balance

As the feed gas passes over the catalyst bed it reacts. The moles of nitrogen, hydrogen and ammonia change. If N is the total molar flow over the catalyst bed then,

$$N_i = x_i \times N \quad (3)$$

N<sub>i</sub> is the flow rate of individual component over the bed. For a packed bed the change in moles of any component per unit time over a differential volume of bed is

$$\frac{dN_i}{dV} = R_i \quad (4)$$

The change of moles of nitrogen per unit time over a differential volume of bed is

$$\frac{dN_{N_2}}{dV} = -R_{N_2} \quad (5)$$

$$\frac{dN_{N_2}}{dV} = -R_{N_2} = \frac{1}{2} R_{NH_3} \quad (6)$$

The change in molar concentration of nitrogen over a differential volume of bed is

$$\frac{dx_{N_2}}{dV} = \frac{\left(-\frac{1}{2}R_{NH_3}\right) - (x_{N_2} \frac{dN}{dV})}{N} \quad (7)$$

The change in molar concentrations of hydrogen and ammonia over a differential volume of bed are

$$\frac{dx_{H_2}}{dV} = \frac{\left(-\frac{1}{3}R_{NH_3}\right) - (x_{H_2} \frac{dN}{dV})}{N} \quad (8)$$

$$\frac{dx_{NH_3}}{dV} = \frac{(R_{NH_3}) - (x_{NH_3} \frac{dN}{dV})}{N} \quad (9)$$

### C. Energy Balance (Gunorubon & Raphael, 2014)

The change in temperature of gas over an infinitesimal catalyst bed is

$$\frac{dT}{dV} = \frac{R_{N_2} * (-\Delta H_{RT})}{N * C_{p,mix}} \quad (10)$$

## II. DETERMINATION OF PARAMETERS

### A. Specific Heat Capacity

(Gunorubon & Raphael, 2014)

The heat capacities of the components of the reactant gases

were obtained with the expression:

$$C_{p_i} = 4.1884(a_i + b_i T + c_i T^2 + d_i T^3) \quad (11)$$

(Refer Table 1, Page 10)

The heat capacity of the ammonia is given by,

$$C_{p_{NH_3}} = (6.5846 - 0.61251 \times 10^{-2} T + 0.23663 \times 10^{-5} T^2 + 1.5981 \times 10^{-9} T^3 + 96.1678 - 0.067571 P + (0.2225 + 1.6847 \times 10^{-4} P) T + (1.289 \times 10^{-4} - 1.0095 \times 10^{-7} P) T^2) \quad (12)$$

### B. Effectiveness Factor ( $\eta$ )

(Gunorubon & Raphael, 2014)

To investigate the effects of temperature and density of the catalyst interior and the difference between these parameters with those of the catalyst surface, an effectiveness factor called  $\eta$  has been defined. The general form of the equation defining this effectiveness factor has been given below.

$$\eta = b_0 + b_1 T + b_2 X + b_3 T^2 + b_4 X^2 + b_5 T^3 + b_6 X^3 \quad (13)$$

(Refer Table 2, Page 10)

### C. Equilibrium Constant ( $K_a$ )

The equilibrium constant was obtained using the expression in (Gunorubon & Raphael, 2014)

$$\log K_a = \left( -2.69112 \log T - 5.51925 \times 10^{-5} T + 1.848863 \times 10^{-7} T^2 + \frac{2001.6}{T} + 2.689 \right) \quad (14)$$

### D. Rate Constant ( $k$ )

The rate constant values were obtained using Arrhenius relation with values for synthesis relation obtained from (Gunorubon & Raphael, 2014)

$$k = k_0 \exp\left(\frac{-E}{RT}\right) \quad (15)$$

### E. Component Fugacity Coefficient

The fugacity coefficients for all the components were determined using the expressions given by (Ukpaka & Izonowei, 2017) as

$$\phi_{H_2} = \left( \exp\left( \exp(-3.802T^{0.125} + 0.541)P - \exp(-0.1263T^{0.5} - 15.98)P^2 + \left( 300 \left( \exp(-0.011901T - 5.941) \left( \exp\left(\frac{P}{300}\right) \right) \right) \right) \right) \right) \quad (16)$$

$$\phi_{N_2} = 0.93431737 + 0.2028538 \times 10^{-3} T + 0.295896 \times 10^{-3} P - 0.270727 \times 10^{-6} T^2 + 0.4775207 \times 10^{-6} P^2 \quad (17)$$

$$\phi_{NH_3} = (0.1438996 + 0.2028538 \times 10^{-3} T + 0.4487672 \times 10^{-3} P - 0.1142945 \times 10^{-5} T^2 + 0.276121 \times 10^{-6} P^2) \quad (18)$$

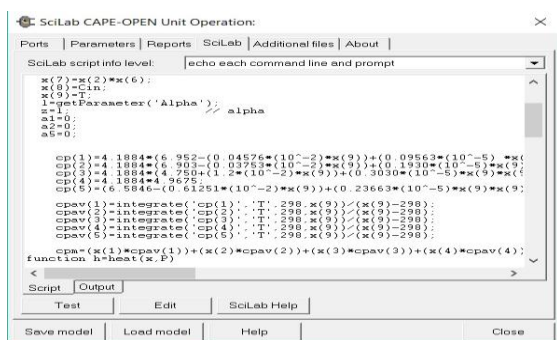
### III. SIMULATION

The topography of the process used in the referred paper was simulated. This flowsheet closely represents an industrial unit. Araujo et al simulated this flowsheet using Aspen Plus®. In this work the flowsheet was simulated using COFE (Cape Open Flowsheet Environment) Simulator.

The catalytic bed in the reference flowsheet were replaced by our own PFR models which were designed using SciLab. The designed PFR models were incorporated in SciLab unit operation of COFE (Cape Open Flowsheet Environment) Simulator

### IV. MODELLING OF THE REACTOR

A 3-Bed PFR was modelled using the Scilab Unit operation. Modelling of the reactor was done by using all the necessary equations mentioned in the above section. The equations were written as a part of the code in Scilab and the program was run accordingly. The code for a particular bed was used for all three beds and introduced in the Scilab Unit Operation in COFE Simulator.



```

SciLab script info level: [echo each command line end prompt]
x(7)=x(2)*x(6);
x(8)=Cln;
x(9)=T;
x=getParameter('Alpha'); alpha
a1=0;
a2=0;
a5=0;
cp(1)=4.1884*(6.952-(0.04576*(10^-2)*x(9))+(0.09563*(10^-5)*x(9)^2)-(0.0375*(10^-3)*x(9)^3)+(0.1930*(10^-5)*x(9)^4);
cp(3)=4.1884*(4.750+(1.2*(10^-2)*x(9))+(0.3030*(10^-5)*x(9)^2)-(0.1930*(10^-3)*x(9)^3);
cp(4)=4.1884*9675;
cp(5)=(6.5846-(0.61251*(10^-2)*x(9))+(0.23663*(10^-5)*x(9)^2)-(0.1930*(10^-3)*x(9)^3);
cpav(1)=integrate('cp(1)',T,298,x(9))/(x(9)-298);
cpav(2)=integrate('cp(2)',T,298,x(9))/(x(9)-298);
cpav(3)=integrate('cp(3)',T,298,x(9))/(x(9)-298);
cpav(4)=integrate('cp(4)',T,298,x(9))/(x(9)-298);
cpav(5)=integrate('cp(5)',T,298,x(9))/(x(9)-298);
cpa=(x(1)*cpav(1))+x(2)*cpav(2)+x(3)*cpav(3)+x(4)*cpav(4);
function h=heat(x,P)
    
```

Fig. 1: A part of the code in Scilab unit operation

### V. ENERGY OPTIMIZATION

When modelled PFRs were incorporated in the referred topography and simulated, the Heat Exchanger duties were as follows:

$$H-501 = 8 \text{ MW} \quad H-583 = 45.56 \text{ MW}$$

An energy optimization was carried out in the flow sheet. Pinch temperature analysis was done considering the necessary hot and cold streams that participated in the heat exchange. The feed composition was altered to ensure the maximum output of Argon (inert) in stream number 25.

This led to the H-501 heat exchanger duty to rise to 18 MW producing a high quality 22000 kg/h of steam at 40.5°C superheat and at a high pressure of 35 bars.

The H-583 heat exchanger duty reduced to 26.4 MW which led to the requirement of the cooling water to go down to 600000 kg/h (which was initially 700000kg/h)

This was done for different values of flow rates of the feed. The figures depicting the energy optimized flow sheet and the corresponding stream data is shown below:

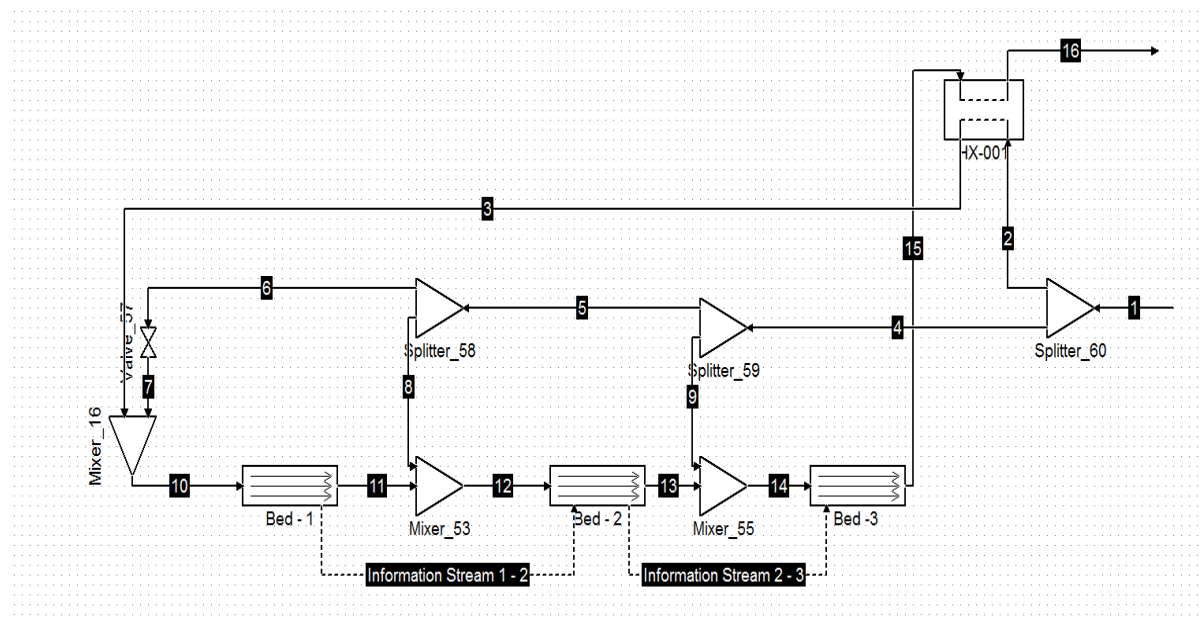


Fig. 2: Scilab Unit Operation – GUI Model

Stream	1	2	3	4	5	6	7	8
Final Conversion								
Pressure	206.957	206.957	206.957	206.957	206.957	206.957	203.957	206.957
Temperature	275.036	275.036	438.776	275.036	275.036	275.036	275.055	275.036
Flow rate	296033	148017	148017	148017	74008.3	46129.4	46129.4	27878.9
Mole frac Hydrogen	0.619973	0.619973	0.619973	0.619973	0.619973	0.619973	0.619973	0.619973
Mole frac Nitrogen	0.2774	0.2774	0.2774	0.2774	0.2774	0.2774	0.2774	0.2774
Mole frac Methane	0.00602568	0.00602568	0.00602568	0.00602568	0.00602568	0.00602568	0.00602568	0.00602568
Mole frac Argon	0.00368112	0.00368112	0.00368112	0.00368112	0.00368112	0.00368112	0.00368112	0.00368112
Mole frac Ammonia	0.0929201	0.0929201	0.0929201	0.0929201	0.0929201	0.0929201	0.0929201	0.0929201

Table 3(i): Stream Report (Fig 2)

9	10	11	12	13	14	15	16	Information Stream 1 - 2	Information Stream 2 - 3	Unit
								0.113421	0.260723	-
Material properties										
206.957	203.957	202.957	202.957	201.957	201.957	200.957	200.957			bar
275.036	400.116	461.449	437.887	494.428	438.674	480.818	396.576			°C
74008.3	194146	194146	222025	222025	296034	296034	296034			kg / h
0.619973	0.619973	0.56431	0.571683	0.498965	0.532233	0.465011	0.465011			
0.2774	0.2774	0.26332	0.265185	0.246791	0.255206	0.238203	0.238203			
0.00602568	0.00602568	0.00640681	0.00635633	0.00685424	0.00662645	0.00708673	0.00708673			
0.00368112	0.00368112	0.00391396	0.00388312	0.00418729	0.00404813	0.00432932	0.00432932			
0.0929201	0.0929201	0.162049	0.152892	0.243202	0.201886	0.28537	0.28537			

Table 3(ii): Stream Report (Fig 2)

The pressure drop across each bed was assumed to be 1 bar, this assumption was made on the basis of the referred paper (Araújo & Skogestad, 2008)

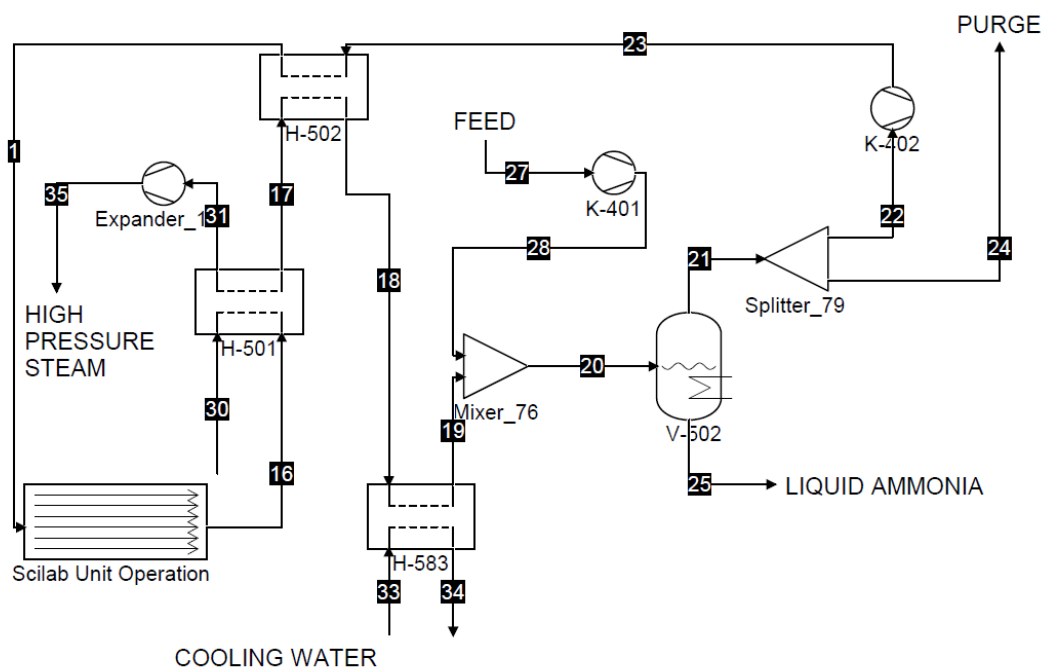


Fig 3: Energy Optimized Flow Sheet

Stream	1	16	17	18	19	20	21	22	23
Pressure	206.957	200.957	200.957	199.957	199.957	196.284	200.284	200.284	207.957
Temperature	275.036	396.576	319.806	65.8375	30	39.8435	20	20	29.855
Flow rate	296033	296034	296034	295588	295588	366572	296025	295995	295995
Mole frac Hydrogen	0.619973	0.465011	0.465011	0.465374	0.465374	0.539787	0.619974	0.619974	0.619974
Mole frac Nitrogen	0.2774	0.238203	0.238203	0.237646	0.237646	0.241164	0.277395	0.277395	0.277395
Mole frac Methane	0.00602568	0.00708673	0.00708673	0.00708565	0.00708565	0.00535193	0.00602635	0.00602635	0.00602635
Mole frac Argon	0.00368112	0.00432932	0.00432932	0.0043343	0.0043343	0.00331254	0.00368388	0.00368388	0.00368388
Mole frac Ammonia	0.0929201	0.28537	0.28537	0.285561	0.285561	0.210384	0.0929203	0.0929203	0.0929203
Mole frac Water									

Table 4(i): Stream Report (Fig 3)

24	25	27	28	30	31	33	34	35	Unit
200.284	200.284	23.1	196.284	35	35	10	10	0.4	bar
20	20	17	343.834	25	282.416	15	50.141	77.6913	°C
29.6025	70547.5	70984.5	70984.5	22000	22000	600000	600000	22000	kg / h
0.619974	0.0171666	0.748035	0.748035						
0.277395	0.00503045	0.251012	0.251012						
0.00602635	0.000956383	0.000500023	0.000500023						
0.00368388	0.000892341	0.000453113	0.000453113						
0.0929203	0.975954	0	0						
				1	1	1	1	1	

Table 4(ii): Stream Report (Fig 3)

## VI. PROFIT ANALYSIS

The results that were achieved by the analysis of change in parameters with respective changes in the inlet flow rates were used to calculate the net operational profit for all the inlet flow rates. This helped us to analyse how the flow rates affect the earnings by the process. The parameters taken into consideration are:

- 1) Net ammonia flow at the outlet of the flash distillation unit.
- 2) Amount of feed at the inlet.
- 3) Amount of purge.
- 4) The total duty required by the 2 compressors.
- 5) Utilities that include:
  - a) Steam produced – positive utility.
  - b) Amount of cooling water required – negative utility.

The Operational Profit is calculated by the formula: (Araújo & Skogestad, 2008)

$$P = \$_{\text{prod}} (x_{\text{NH}_3} F_{\text{prod}}) + \$_{\text{purge}} F_{\text{purge}} + \$_{\text{steam}} F_{\text{steam}} - \$_{\text{gas}} F_{\text{gas}} - \$_{\text{WS}} (W_{\text{K-401}} + W_{\text{K-402}}) - \$_{\text{CW}} F_{\text{CW}} \quad (19)$$

Where  $x_{\text{NH}_3}$  is the product purity,  $F_{\text{steam}}$  is the steam generation in kg/h and  $F_{\text{CW}}$  is the amount of cooling water required in  $\text{m}^3/\text{h}$ .

Note that P is the operational profit and does not include other fixed costs or capital costs.

The prices are

$$\begin{aligned} \$_{\text{prod}} &= 0.200\$/\text{kg}, \\ \$_{\text{purge}} &= 0.010\$/\text{kg}, \\ \$_{\text{steam}} &= 0.017\$/\text{kg}, \\ \$_{\text{gas}} &= 0.080\$/\text{kg}, \\ \$_{\text{WS}} &= 0.040\$/\text{unit and}, \\ \$_{\text{CW}} &= 0.137366/\text{m}^3. \quad (\text{Ulrich \& Vasudevan, 2006}) \end{aligned}$$

The above formula gives us the profit in \$/h.

## VII. RESULTS AND DISCUSSIONS

After optimising the flow sheet for various flow rates, the following results were observed:

- 1) There is a fixed pattern in the temperatures of the respective beds for different flow rates. It is quite evident from the temperature profile along the beds shown below. (Fig 4)

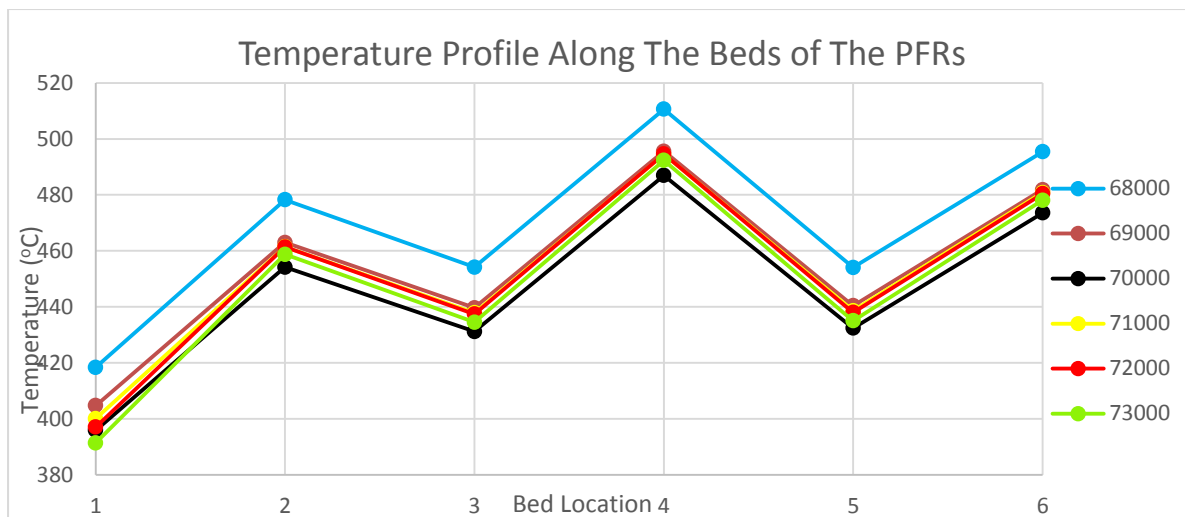


Fig 4: Temperature Profile

Here, on the x-axis, the scale indicates:

- 1 – Bed 1 inlet
- 2 – Bed 1 outlet
- 3 – Bed 2 inlet
- 4 – Bed 2 outlet
- 5 – Bed 3 inlet
- 6 – Bed 3 outlet

From the plot, it is observed that the temperature profile for the feed flow rate of 70000 kg/h behaves a bit differently from the other flow rates across the bed. The temperature at the outlet of bed 2 for the feed

flow rate of 68000 kg/h goes beyond 500°C, which is generally the upper limit for a reactor temperature in an ammonia synthesis process. This is because the inlet temperature of the reactor is very high.

2) It is also observed that the ammonia production increases as we increase the feed flow rates.

3) The Operational Profit (P), on an overall basis, increases as we increase the feed flow rate. The plot of P vs Flow Rates is shown below: (Fig 5)

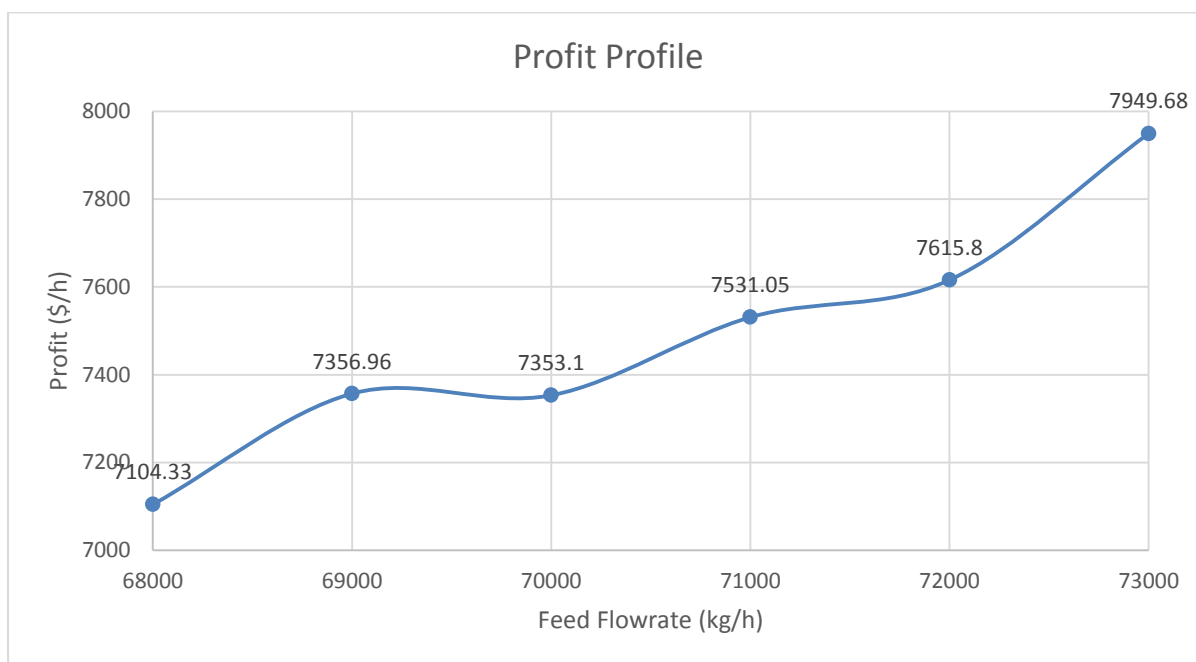


Fig 5: Profit v/s Flowrate

4) It can be noticed that the Profit sees an almost-stagnant zone between the flow rates of 69000 kg/h to 70000 kg/h. The major reason for this anomaly is the unusual behaviour of the temperature along the bed 1 for the 70000 kg/h flow rate. This unexpected drop in the temperatures results in the reduction of the overall conversion of the process, which, in turn, produces lesser ammonia than expected hence, limiting the profit.

Another conclusion that can be made from this information is that, the profit from the process majorly depends upon the total production of ammonia in the process.

(NOTE: We can see that the amount of steam generated and the cooling water required remain constant throughout. This is because we have taken constant duties across the respective heat exchangers and kept the flow rates constant too in order to obtain more relatable results for the varying flow rates of feed at the inlet. (Table 5)

UO	Parameter	Value	Unit
H-501	Heat exchange	18	MW
H-583	Heat exchange	26.3912	MW

Table 5: Heat Exchanger Duties

5) We can also see that the conversions in each and every subsequent case increase slightly. This is basically due to relative composition of ammonia entering the reactor inlet in each case. We experience these changes because we change the conditions of the flash distillation units in each and every case to balance out the inerts entering the process via the feed in order to avoid accumulation (refer Table). This is because, the accumulation of inerts in the process would keep on reducing the overall conversion of the process over time and this would result in reduced profits because of lesser ammonia at the outlet. (Table 6).

Because more amount of ammonia is removed in each and every case, lesser ammonia goes into recycle and hence the molar composition of ammonia at the reactor inlet drops.

Since the molar composition of ammonia in the inlet drops, it forces the equilibrium to shift forward, giving us a larger conversion in return.

Flow rate (kg/h)	Mole Fraction Of Ammonia Entering The Reactor	Flash Conditions		Conversion
		Temperature (°C)	Pressure (bar)	
68000	0.096	20.25	199	0.379
69000	0.0957	21	200.284	0.384
70000	0.094	20.4	200.284	0.363
71000	0.0929	20	200.284	0.397
72000	0.09027	19	201.284	0.399
73000	0.0878	18.2	203.284	0.402

Table 6: Conversion with Different Flowrates

Constants	Component			
	H <sub>2</sub>	N <sub>2</sub>	CH <sub>4</sub>	Ar
a	6.952	6.903	4.75	4.9675
b x 10 <sup>2</sup>	-0.04567	-0.03753	1.2	-
c x 10 <sup>5</sup>	0.095663	0.193	0.303	-
d x 10 <sup>5</sup>	-0.2079	-0.6861	-2.63	-

Table 1: Coefficient for specific heat capacity of gas mixture (Ukpaka & Izonowei, 2017)

Pressure (bar)	b <sup>0</sup>	b <sup>1</sup>	b <sup>2</sup>	b <sup>3</sup>	b <sup>4</sup>	b <sup>5</sup>	b <sup>6</sup>
150	-17.539096	0.07697849	6.900548	-1.08279e-4	-26.42469	4.927648e-8	38.937
225*	-8.2125534	0.03774149	6.190112	-5.354571e-5	-20.86963	2.379142e-8	27.88
300	-4.6757259	0.02354872	4.687353	-3.463308e-5	-11.28031	1.540881e-8	10.46

Table 2: coefficients of effectiveness factor

## REFERENCES

- [1] <https://www.ihs.com/products/ammonia-chemical-economics-handbook.html>
- [2] <https://en.wikipedia.org/wiki/Ammonia#History>
- [3] <https://en.wikipedia.org/wiki/Ammonia#Properties>
- [4] [http://nano.tau.ac.il/mncf/images/MSDS/NH3\\_gas.pdf](http://nano.tau.ac.il/mncf/images/MSDS/NH3_gas.pdf)
- [5] [http://www.rmtech.net/uses\\_of\\_ammonia.html](http://www.rmtech.net/uses_of_ammonia.html)
- [6] <http://www.chemguide.co.uk/physical/equilibria/haber.html>
- [7] Araújo, A., & Skogestad, S. (2008). Control structure design for the ammonia synthesis process. *Computers & Chemical Engineering*, 32(12), 2920–2932. <https://doi.org/10.1016/j.compchemeng.2008.03.001>
- [8] Bland, M. J. (2015). Optimisation of an Ammonia Synthesis, (June).
- [9] Dyson, D. C., & Simon, J. M. (1968). A kinetic expression with diffusion correction for ammonia synthesis on industrial catalyst. *Industrial and Engineering Chemistry Fundamentals*, 7(4), 605–610. <https://doi.org/10.1021/i160028a013>
- [10] Gunorubon, A. J., & Raphael, R. N. (2014). Simulation of an Ammonia Synthesis Converter. *Canadian Journal of Pure and Applied Sciences*, 8(2), 2913–2923. [https://doi.org/10.1016/0009-2509\(65\)85017-5](https://doi.org/10.1016/0009-2509(65)85017-5)
- [11] Ukpaka, C. P., & Izonowei, T. (2017). Model Prediction on the Reliability of Fixed Bed Reactor for Ammonia Production. *Chemistry International*, 3(31), 46–57. Retrieved from [www.bosaljournals/chemint/](http://www.bosaljournals/chemint/)
- [12] Ulrich, G. D., & Vasudevan, P. T. (2006). How to estimate utility costs. *Chemical Engineering*, 113(4), 66–69.